

Dynamics of surface profile evolution through surface diffusion

M. V. Ramana Murty and B. H. Cooper

Cornell University, Laboratory of Atomic and Solid State Physics, Ithaca, New York 14853

(Received 29 April 1996)

We have studied the evolution, mediated by surface diffusion, of periodic corrugations on a surface using Monte Carlo simulations on a solid-on-solid (SOS) model. Above the roughening temperature T_R , for both unidirectional and bidirectional sinusoidal corrugations of wavelength L , the amplitude h decays exponentially with time $h/h_0 \approx \exp(-\alpha t)$, with t/L^4 scaling in agreement with Herring-Mullins theory. Below the roughening temperature, there is a gradual transition to a power-law decay of the amplitude as the temperature is lowered. The wavelength scaling varies with the substrate temperature and the periodicity of the corrugation in the two orthogonal transverse directions. Well below T_R , the amplitude in unidirectional sinusoidal corrugations evolves with time according to $h/h_0 \approx (1 + \lambda t)^{-1}$, with t/L^5 scaling for diffusion-limited kinetics, in agreement with the theory of Ozdemir and Zangwill [Phys. Rev. B **42**, 5013 (1990)]. In bidirectional sinusoidal corrugations, profile decay is driven by a combination of line-tension and step-step entropic repulsion, in agreement with the theory of Rettori and Villain [J. Phys. (Paris) **49**, 257 (1988)]. [S0163-1829(96)07439-5]

An important problem in crystal growth is the continuum description of surface morphology in terms of roughening processes such as the random arrival of atoms, strain and diffusion bias, and smoothing processes such as surface and bulk diffusion and evaporation-condensation. Surface diffusion is the dominant mechanism of relaxation during thin-film growth of many materials. A mathematical framework for the continuum description of relaxation was provided by Herring¹ and later developed by Mullins.² For the canonical problem of the evolution of an imprinted sinusoidal profile of wavelength L , this predicts a shape-preserving solution with an exponential decay of the amplitude with time t and t/L^4 scaling. This has been verified both experimentally³⁻⁵ and in Monte Carlo simulations⁵⁻⁸ above the surface-roughening transition temperature T_R . Below T_R , the associated equations become singular due to the cusp in the surface free energy at low index orientations.

Both analytic⁹⁻¹⁶ and Monte Carlo^{6,8,17-20} techniques have been used to study profile evolution below T_R . Analytical models describe surface relaxation below T_R to be driven by step-step interactions and line tension. For a unidirectional sinusoidal profile, they predict the appearance of a flat top and a power-law decay of the amplitude with t/L^5 scaling for diffusion-limited kinetics.¹¹ Experiments on periodic profiles on Ni and Si(001) have shown the development of a flat top, but the amplitude evolution appears to follow t/L^4 scaling.^{4,21} Monte Carlo simulations have reproduced the t/L^4 scaling close to but below T_R (Refs. 8 and 19). For a bidirectional sinusoidal profile, the amplitude decay is expected to follow t/L^3 scaling for diffusion-limited kinetics.⁹ Annealing of rough surfaces of Cu(111) produced by growth²² and of TiO₂(110) (Ref. 23) and Ge(001) (Ref. 24) produced by ion bombardment has yielded results consistent with amplitude decay following t/L^n scaling, with n taking the values of 3 (short-time behavior), 4, and 2.2 for Cu(111), TiO₂, and Ge(001), respectively. Thus we see a wide variation in the time and wavelength dependence of the profile evolution. As many crystal processing steps occur well below T_R , it is of interest to determine the onset and nature of low-temperature profile evolution.

In this Brief Report, we discuss Monte Carlo simulations on a solid-on-solid (SOS) model of surface profile evolution above and below the surface-roughening temperature. As the substrate temperature is lowered from above to below T_R , there is a gradual transition from an exponential decay to a power-law decay of the amplitude. The wavelength scaling varies with the substrate temperature and the periodicity of the corrugation in the two orthogonal transverse directions. Well below T_R , the amplitude in unidirectional sinusoidal corrugations evolves with time according to $h/h_0 \approx (1 + \lambda t)^{-1}$, with t/L^5 scaling for diffusion-limited kinetics in agreement with analytic theory.¹¹ In bidirectional sinusoidal corrugations, profile decay is driven by a combination of line-tension and step-step entropic repulsion, also in agreement with analytic theory.⁹

The SOS model is described by the Hamiltonian

$$H = \frac{\varepsilon}{2} \sum_{ij} |h_i - h_j|, \quad (1)$$

where h_i is the height at site i and ε is the bond energy. The simulations were performed on a square lattice with the sum limited to nearest neighbors. Periodic boundary conditions were employed in the transverse directions. The roughening transition temperature T_R for this model is $k_B T_R / \varepsilon = 0.62$.²⁵ The only interactions between steps in this SOS model are statistical. The free energy per unit projected surface area G can be expanded in terms of the slope h_x as

$$G = G_0 + G_1 |h_x| + \frac{1}{2} G_2 h_x^2 + \frac{1}{3} G_3 |h_x|^3 + \dots \quad (2)$$

For $T > T_R$, the coefficients of odd powers $G_1 = G_3 = \dots = 0$.^{2,9} For $T < T_R$, current models of surfaces predict the coefficient G_2 of the quadratic term to vanish, and the condition of noncrossing of steps gives rise to the cubic term in the projected surface free energy.²⁶

The Monte Carlo simulations were performed in $(2+1)D$ with conservative dynamics. Each step consists of picking a site at random and making a move to an adjacent site with probability

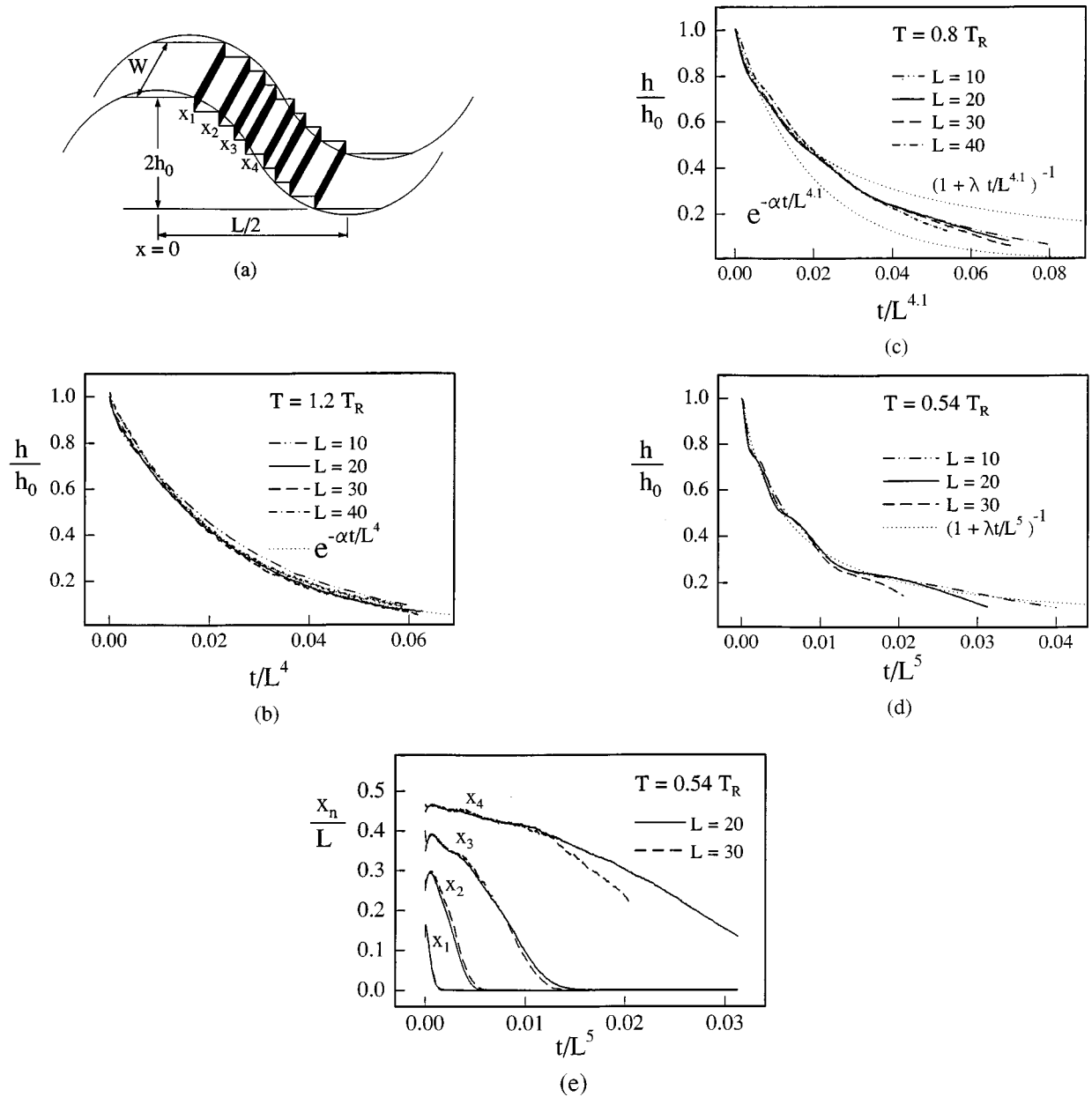


FIG. 1. (a) A discretized unidirectional sinusoidal corrugation with an amplitude $h_0=4$ units. The evolution of the amplitude h/h_0 as a function of scaled time t/L^n at (b) $T=1.2T_R$, (c) $T=0.8T_R$, and (d) $T=0.54T_R$. The amplitude is defined as the average height at one or two rows at the extrema of the initial sinusoidal pattern. The data are averaged over at least 5000 columns. Also shown are the functions $\exp(-\alpha t/L^n)$ and $(1+\lambda t/L^n)^{-1}$, where α and λ were chosen to give good fits to the initial 25% of the decay in amplitude. (e) The variation in scaled step positions shown as a function of t/L^5 for the wavelengths of $L=20$ and 30 lattice units at $T=0.54T_R$.

$$p = \begin{cases} \frac{1}{4} \exp(-\Delta E/k_B T), & \Delta E > 0 \\ \frac{1}{4}, & \Delta E \leq 0 \end{cases} \quad (3)$$

where ΔE is the difference in binding energy between the present site and the new (adjacent) site. The approach to equilibrium was investigated for unidirectional and bidirectional sinusoidal corrugations. At low temperatures, the average position of steps was followed by determining the number of atoms at each level. This introduces an error due to incomplete cancellation of adatom and vacancy concentrations, but this is deemed sufficiently small to not affect the conclusions drawn here. The size of the surface ranged from 10^4 to 10^5 columns. It is noted that the width W in the direc-

tion of the groove in unidirectional corrugations [Fig. 1(a)] must be sufficiently large to allow for many step-step collisions. A nonmonotonic change in the rate of amplitude decay was observed as W was increased from very small (essentially no collisions over the whole width) to large values (few to several collisions). A width of 1000 lattice units was used for the simulations below the roughening temperature.

The time evolution of the amplitude in unidirectional sinusoidal corrugations was studied at five different temperatures ranging from $T=0.54T_R$ to $1.2T_R$ for the wavelengths of $L=10-40$ units. The initial amplitude h_0 was four units. The amplitude h represents an average over either one or two rows (perpendicular to the corrugation direction) at the extrema of the starting sinusoidal profile. The data shown are

averaged over at least 5000 columns. Figures 1(b)–1(d) show the amplitude decay at three different temperatures. Also shown are the functions $h/h_0 = \exp(-\alpha t/L^n)$ and $h/h_0 = (1 + \lambda t/L^n)^{-1}$. It is noted that the parameters α and λ were chosen to give good fits to the initial 25% of the decay. At $T = 1.2T_R$ [Fig. 1(b)], the decay is seen to be exponential, with a t/L^n scaling, $n = 4.0 \pm 0.1$, in agreement with Herring-Mullins theory.² Assuming the effective activation energy of $2\varepsilon + \varepsilon_d$ (sum of adatom formation and migration energy) in the coefficient α , we get $G_2 = 1.24\varepsilon$. As the temperature is lowered, we observe a gradual transition from an exponential decay to a power-law decay of the amplitude. This does not agree with the prediction of a linear decay of the amplitude below T_R .¹³ At $T = 0.8T_R$, the scaling is still of the form t/L^n , $n = 4.1 \pm 0.1$, in agreement with earlier Monte Carlo simulations [Fig. 1(c)].^{8,19} However, the decay function deviates from the exponential form. At $T = 0.54T_R$, the amplitude decay [Fig. 1(d)] follows the power law, as predicted for relaxation driven by step-step entropic repulsion.¹¹ Also the wavelength scaling exponent $n = 5$ gives a good fit over a significant portion of the decay (up to $h \approx 0.25h_0$), as expected for diffusion-limited kinetics.¹¹ The scaling is not as good toward the end when only one pair of steps is left. This may be due to finite-size effects from larger step separation as noted above. The plateaus in Fig. 1(d) correspond to integer heights h . The plateaus would be less prominent for higher values of the initial amplitude h_0 .

The decay proceeds through the contact of unlike steps at the extrema. This leads to formation of islands and their subsequent evaporation onto the terrace.⁹ Figure 1(e) shows the average position of individual steps during the profile evolution at $T = 0.54T_R$. For the steps at the extrema, we define an effective step position in terms of the number of atoms or vacancies remaining. We see that all steps move toward the center and the low index facet at the top grows as each pair of steps annihilate. The scaled step positions show t/L^5 scaling, which indicates that the shape of the evolving profile follows this scaling. It is also interesting to note the sudden change in the step velocities when the steps at the extrema vanish, in agreement with the description in analytic theory.¹¹ The entropic repulsion faced by the next to last step at the extrema decreases rapidly on one side, resulting in the sudden change in velocities of all steps.

The evolution of bidirectional sinusoidal corrugations described by the envelope

$$h(x, y, 0) = h_0 \sin\left(\frac{2\pi x}{L}\right) \sin\left(\frac{2\pi y}{L}\right) \quad (4)$$

was also investigated. The wavelengths in the range $L = 16$ – 60 lattice units were again followed at different temperatures from $T = 0.54T_R$ to $1.2T_R$. The initial amplitude h_0 was four units. Above T_R , the amplitude decayed exponentially with time with t/L^4 scaling as expected. Below T_R , profile decay is driven by line tension in addition to step-step entropic repulsion. Figure 2 shows the variation of amplitude at $T = 0.54T_R$ with time scaled by two different wavelength exponents, t/L^5 and t/L^3 . We see that there is no single wavelength scaling exponent valid for all wavelengths. For example, at short wavelengths ($L = 16, 20$), $n \approx 5$ gives a reasonable fit, while a similar exercise at the longest wave-

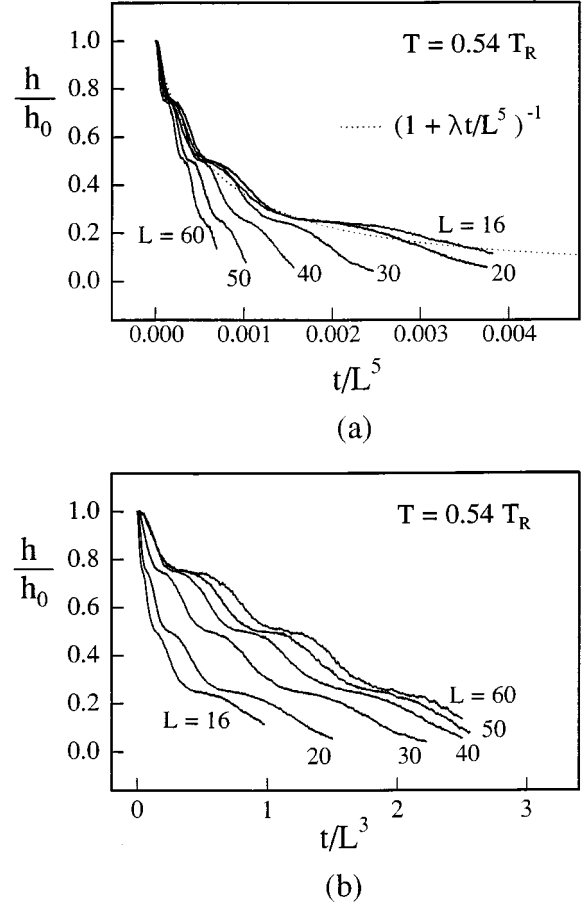


FIG. 2. Evolution of the amplitude h/h_0 with scaled time t/L^n , $n = 5$ and 3 at $T = 0.54T_R$ for wavelengths from $L = 16$ to 60 lattice units in bidirectional sinusoidal corrugations. The data are averaged over at least 500 columns, except at $L = 60$, where it is averaged over 200 columns.

lengths ($L = 40, 50$, and 60) yields $n \approx 3.8$. This shift can be understood qualitatively in terms of the line tension and step-step entropic contributions to the excess step chemical potential.^{9,27} For a fixed initial amplitude, steps are more closely spaced at short wavelengths, giving rise to a large step-step entropic term. This leads to a decay similar to that of unidirectional profiles. At large wavelengths the line tension dominates for the islands at the extrema. The analytically predicted form of the decay in this limit is $h - h_0 \sim -\beta t/L^3$.⁹ The simulations show a trend toward $n = 3$ as the wavelength increases. An exponential decay of the amplitude with t/L^3 scaling has been observed below T_R in this SOS model, but with different dynamics.²⁰

One effect not included in analytic models is the interaction between opposite steps at the extrema in unidirectional sinusoidal corrugations.^{6,11,20} These models strictly describe the evolution of a corrugation with only one type of step. Evolution of a half-sinusoidal profile (corresponding to $L = 20$, $h_0 = 4$ and employing screw periodic boundary conditions) with only one type of step has shown that the steps at the extrema move more slowly than their counterparts in the full sinusoidal profile (using the definition above of effective step position). This clearly shows that the island decay must be taken into account for a determination of the absolute rate

of decay. This phenomenon of step-antistep annihilation is analogous to the single step to double step transition on vicinal surfaces.²⁸

We discuss certain features regarding the details of the simulation. The starting surface configuration is a discretized sine wave with straight steps (in unidirectional gratings), and one would expect a finite time for the steps to develop thermal fluctuations. Figure 1(e) shows the rapid readjustment of step positions at the beginning of decay. This shows that equilibration time is short compared to the total time of decay and hence is not a major factor in the observed time evolution of the amplitude. Another feature is the rather large slopes of the profiles in the simulations. The analytical theory is developed in the limit of small slopes, yet we get an excellent agreement with analytical expressions of decay. This may come from two sources. First, the higher-order terms [$O(h_x^4)$] in the projected surface free energy may be small. The other is the assumption of infinite vertical diffusion in the dynamics of the SOS model. The small slope approximation in analytical theory comes from considering only mass transport in the transverse directions, and is equivalent to the assumption of infinite vertical diffusion. Hence a simplifying step in the dynamics of the SOS model might be aiding us in making a comparison to analytical expressions.

The decay of sinusoidal profiles followed diffusion-limited kinetics since there was no step-attachment barrier.²⁹ In the other extreme of interface-limited decay amplitude evolution follows t/L^4 scaling for unidirectional profiles¹¹ and t/L^2 scaling for bidirectional profiles. Hence, surfaces evolving through surface diffusion below the roughening temperature may show amplitude following t/L^n scaling, with n ranging from 2 to 5.

In conclusion, we have studied the evolution of unidirectional and bidirectional sinusoidal corrugations above and below the roughening transition temperature T_R on a SOS model using Monte Carlo simulations. Above T_R , the amplitude decays exponentially with time, in agreement with Herring-Mullins theory.² Below the roughening temperature, there is a gradual transition to a power-law decay of the amplitude as the temperature is lowered. The wavelength scaling varies with the substrate temperature and the periodicity of the corrugation in the two orthogonal transverse directions. Well below T_R , the amplitude in unidirectional sinusoidal corrugations evolves with time according to $h/h_0 \approx (1 + \lambda t)^{-1}$, with t/L^5 scaling for diffusion-limited kinetics in agreement with analytic theory.¹¹ In bidirectional sinusoidal corrugations, profile decay is driven by a combination of line-tension and step-step entropic repulsion, also in agreement in analytic theory.⁹

We would like to thank Professor J. P. Sethna for suggesting the problem and acknowledge several enlightening discussions with Jim Sethna, Eugene Kolomeisky, Jack Blakely, Chris Henley, and Mike Dubson. This work was supported by NSF under Grant No. GER 9022961 and Cornell University Materials Science Center under Grant No. DMR 9121654.

Note added in proof. We have performed kinetic Monte Carlo simulations and they yield the same results described in this paper. In writing the probabilities of jumps [Eq. (3)], we have taken the energy of the transition state between any two neighboring sites i and j to be ε_d higher than the higher of the two states i and j . This is irrespective of the binding at sites i and j .

-
- ¹C. Herring, in *Structure and Properties of Solid Surfaces*, edited by R. Gomer and C. S. Smith (University of Chicago Press, Chicago, 1952), p. 1.
- ²W. W. Mullins, in *Metal Surfaces: Structure, Energetics and Kinetics*, edited by N. A. Gjostein and W. D. Robertson (American Society for Metals, Metals Park, OH, 1963), p. 99.
- ³J. M. Blakely and H. Mykura, *Acta Metall.* **10**, 565 (1962); P. S. Maiya and J. M. Blakely, *J. Appl. Phys.* **38**, 698 (1967).
- ⁴K. Yamashita, H. Bonzel, and H. Ibach, *Appl. Phys.* **25**, 231 (1981).
- ⁵Z. Jiang and C. Ebner, *Phys. Rev. B* **40**, 316 (1989).
- ⁶W. Selke and P. M. Duxbury, *Phys. Rev. B* **52**, 17 468 (1995).
- ⁷W. Selke and P. M. Duxbury, *Z. Phys. B* **94**, 311 (1994).
- ⁸P. C. Searson, R. Li, and K. Sieradzki, *Phys. Rev. Lett.* **74**, 1395 (1995).
- ⁹A. Rettori and J. Villain, *J. Phys. (Paris)* **49**, 257 (1988).
- ¹⁰F. Lancon and J. Villain, *Phys. Rev. Lett.* **64**, 293 (1990).
- ¹¹M. Ozdemir and A. Zangwill, *Phys. Rev. B* **42**, 5013 (1990).
- ¹²H. Spohn, *J. Phys. I (France)* **3**, 69 (1993).
- ¹³J. Hager and H. Spohn, *Surf. Sci.* **324**, 365 (1995).
- ¹⁴N. C. Bartelt, J. L. Goldberg, T. L. Einstein, and E. D. Williams, *Surf. Sci.* **273**, 252 (1992).
- ¹⁵H. P. Bonzel and W. W. Mullins, *Surf. Sci.* **350**, 285 (1996).
- ¹⁶E. B. Kolomeisky (unpublished).
- ¹⁷W. Selke and T. Bieker, *Surf. Sci.* **281**, 163 (1993).
- ¹⁸M. A. Dubson and G. Jeffers, *Phys. Rev. B* **49**, 8347 (1994).
- ¹⁹Z. Jiang and C. Ebner, *Phys. Rev. B* **53**, 11 146 (1996).
- ²⁰J. Erlebacher and M. J. Aziz (unpublished).
- ²¹M. E. Keeffe, C. C. Umbach, and J. M. Blakely, *J. Phys. Chem. Sol.* **55**, 965 (1995).
- ²²J.-K. Zuo and J. F. Wendelken, *Phys. Rev. Lett.* **70**, 1662 (1993).
- ²³B. Grossman and P. Piercy, *Phys. Rev. Lett.* **74**, 4487 (1995).
- ²⁴S. J. Chey, J. E. van Nostrand, and D. G. Cahill, *Phys. Rev. Lett.* **53**, 11 146 (1996).
- ²⁵W. J. Shugard, J. D. Weeks, and G. H. Gilmer, *Phys. Rev. Lett.* **41**, 1399 (1978).
- ²⁶J. Y. Tsao, in *Materials Fundamentals of Molecular Beam Epitaxy* (Academic, Boston, 1993), Chap. 6, and references therein.
- ²⁷The excess chemical potential of step n is given by
- $$\mu_n = \frac{4\Omega}{L^2} \left[\frac{G_1}{r_n} + \frac{2}{3} G_3 \left(\frac{1}{l_n^3} - \frac{1}{l_{n-1}^3} \right) + \frac{G_3}{3r_n l_n^2} \right]$$
- where r_n is the radius of step n and $l_n = r_n - r_{n-1}$, and Ω is the atomic volume. The first term is the line tension arising from step curvature, and the next two terms represent the step-step entropic interaction and its curvature dependence. It is assumed that G_1 and G_3 are independent of step orientation.
- ²⁸S. V. Khare, T. L. Einstein, and N. C. Bartelt, *Surf. Sci.* **339**, 353 (1995).
- ²⁹A. Zangwill (private communication).